Journal of Scientific and Technical Research
15 (2) 2025, 99-113
www.publishingindia.com/jstr
https://doi.org/10.21863/jstr/2025.15.2.011

Natural Compounds as Potential Inhibitors of PIK3CG for the Management of Triple-Negative Breast Cancer: A Biocomputational Study

Prashant Kumar Tiwari, Santosh Kumar Mishra and Sanjay Kumar*
Biological and Bio-Computational Lab, Department of Life Science, Sharda School of Bio-Science & Technology, Greater Noida, Uttar Pradesh, India.
*Corresponding Author: sanjay.kumar7@gmail.com; sanjay.kumar7@sharda.ac.in

Abstract: Triple negative breast cancer (TNBC) an aggressive and diverse subtype of breast cancer. Lack of three crucial receptors estrogen, progesterone, and HER2 expression make untreatable now yet, many approaches utilized but no satisfactory results came to manage TNBC. In numbers of treatments strategy chemotherapy, a promising option, while chemoresistance major challenge. In this study, we investigated natural compounds as possible inhibitors of PI3KG, a crucial protein associated with cancer growth and therapy resistance. Molecular docking research revealed that all five tested natural compounds exhibited enhanced binding affinity for PI3KG. Among them Phosmidosine B had the highest affinity, with a docking score of -10.01 kcal/mol and a Glide energy of -60.45 kcal/mol. Emodacidamide E (9.69 kcal/mol; -56.91 kcal/mol), Emodacidamide H (-9.62 kcal/mol; -52.49 kcal/mol), Methylinoscavin D (-9.57 kcal/mol; -58.71 kcal/mol), and 1-hydroxymethyl-8-hydroxy-anthraquinone-3-carboxylic acid (-9.54 kcal/mol; -43.78 kcal/mol) followed. ADME analysis and cytotoxicity prediction showed that all of the chosen compounds had good drug like attributes and safety profiles, which supports their drug properties and low toxicity potential. In conclusion, the significant binding affinities, stable interaction energies, and good ADME and cytotoxicity profiles of these natural compounds, show that they could be good PI3KG inhibitors. Nevertheless, extensive experimental validation is essential to facilitate their further therapeutic advancement.

Keywords: Cytotoxicity profiles, PIK3G, Structural based virtual screening, Triple negative breast cancer, Natural compounds.

I. Introduction

According to GLOBOCAN 2022 reports breast cancer predominant malignancy globally, approximately 2.29 million new cases and 666,103 fatalities, with almost 8.17 million women surviving the disease five years post-diagnosis, while in India, breast cancer results in 192,020 new cases and 98,337 fatalities each year, with a five-year incidence exceeding 526,000 instances. These data underscore the significant worldwide and national impact of breast cancer patients and the ongoing necessity for enhanced prevention, early diagnosis, and treatment strategy (https://www.who.int/). Breast cancer poses extra health burden on female, breast cancer manly classified based on histology and molecular receptor status. In case of histology tumor examine in under microscope and its appearance further subcategories include invasive lobular carcinoma, DCIS, and invasive ductal carcinoma. While receptors status based determined by whether or not ER, PR, and HER2 present. As a result, tumors can be categorized as hormone receptor-positive, HER2-enriched, or triple-negative [1].

TNBC has been identified by the lack of specific estrogen and progesterone receptor expression, additionally absence of HER2 receptor amplification. It was notice that TNBC especially common among Black and pre-menopausal women with downstream and significant psychological and treatment-related issues [2]. Similar to other breast cancer TNBC has biological heterogeneity, leading to different clinical and epidemiological manifestations, but unlike other clinical subtypes, TNBC remains devoid of tumor specific targeted therapeutic agents [3]. Recent studies highlighted several molecular targets in TNBC that can be a promising target to management of its, in a various examples EGFR, VEGF, AR, ERβ, PI3K, mTOR, and AKT are few targets that previously utilized but did not show results as satisfactory as expected [4]. This rapidly growing disease is posing a challenge to the scientific community, and if no promising solution is discovered soon, countless patients may have to lay down their lives. So, it is essential to search for new targets in an immediate basis, researchers now rely on multiple approaches, and one of the most informative is the study of differentially expressed genes (DEGs). DEGs make it possible to distinguish between the genes that are involved in disease and those that are not. Additionally, data from the Gene Expression Omnibus is widely used for this purpose, combined with bioinformatics

tools and web-based pipelines to identify TNBC-specific DEGs. These genes map to key biological pathways that support cancer growth and survival. In a recent analysis, Murtada K. Elbashir and colleagues identified several genes associated with breast cancer, including CDK1, KIF11, CCNA2, TOP2A, ASPM, AURKB, and CCNB2 [5].

The Phosphoinositide-3 kinase gamma (PIK3CG) gene encodes isoform phosphoinositide-3 kinase gamma (PI3KG), which is an isoform of the class I PI3K, it has role in the activation of immune cells and in their chemotaxis and swelling signaling. Although there are many other types of PI3K expressed in most normal tissues [6]. PI3Ks significantly studies in cancer biology because of the significant roles they play in the regulation of cell migration, cell metabolism, cell proliferation, cell survival and cell immune response [7]. PI3Ks are lipid bound kinases that have a catalytic subunit, and a regulatory subunit. PI3Ks are classified into different classes based on their similarities in the major structures, regulatory associations, and sequences. Class IA and IB is further sub-divided into Class I PI3Ks. Class IA PI3Ks consist of p110 catalytic subunits linked with a p85 regulatory subunit, whereas Class IB isoform PI3K isoforms are p110 catalytic subunits with a p101 or p84/p87 regulatory subunit. These regulatory subunits form the structural basis of isoform-specific activation and maintain the catalytic subunits in a low-activity form [8]. PI3Ks control the regulation process of phosphatidylinositol (4,5)-bisphosphate (PIP2) to phosphatidylinositol (3,4,5)-trisphosphate (PIP3) at cellular membranes, that involve intracellular signaling [9]. The downstream signaling pathways control cell survival, proliferation, metabolism, migration, and immunological response and produced PIP3 is a docking site of proteins carrying pleckstrin homology domains, primarily AKT and PDK1. Although PI3K signaling plays a critical role in normal cellular homeostasis by regulating activities of many effectors such as AKT and mTOR, its disregard is linked to cancer development, immunological breakdown, and therapy resistance [10].

PI3K actively utilized as a therapeutic target [11]. Some PI3K inhibitors have already tested preclinical and clinical stages of development. Although this was not the case with the earlier drugs, there are dual PI3K inhibitors such as duvelisib that had been approved to be used in clinical practice but had severe side effects limiting their usage. Highly selective PI3K inhibitors, including ZX-4081, AZD3458, IPI-549 and AZD8154 have demonstrated immunomodulatory and anticancer effects in preclinical studies and in early phase clinical trials in recent times [12].

The use of natural products by traditional medicine has been a practice that has been in existence since time immemorial to treat a wide range of conditions in humans. It is not a secret that bioactive chemicals present in plants, fungus, bacteria, and marine organisms had therapeutic potential long ago [13]. NPs regulate the signaling pathways related to cancer and suppress the aggressiveness of tumors, as well as restrict the growth and spread of cancer cells. This is an indication that NPs possess strong anticancer properties [14]. Some of the naturally occurring compounds, the possible role of which in cancer treatment is well-documented, include Thymoquinone, silibinin, curcumin, honokiol, resveratrol, diosgenin, quercetin, tetrandrine, garcinol, and genistein. [15]. Such compounds possess several promising properties that would enable different safer and more effective approaches to breast cancer treatment in the future, such as the capability of inducing apoptosis, preventing angiogenesis, arresting the cell cycle, and disrupting essential oncogenic signaling pathways. The natural materials can target the treatment of cancer with PI3KG due to their properties [16].

In this study, utilized bio-computation pipeline to identify potential natural candidates to inhibit the PIK3G protein.

II. Experimental Details

A. Protein Optimization

Co-crystal structure of PI3KG retrieved from RCSB PDB (protein data base) (https://www.rcsb.org/), crystal structure (PDB ID: 6GQ7) was determined at 2.84 Å resolution by X-ray diffraction. 3-methyl-1-(oxan-4-yl)-8-pyridin-3-yl-imidazo[4,5-c]quinolin-2-one is bound within the active site of this complex. Native ligands are the inhibitor and provide an idea of how PI3KG changes shape and interacts with other molecules. Using this structural information, the target protein was further refined to ensure it was stable and ready for molecular docking assays.

Co-crystal structure of PI3KG was optimized using protein preparation wizard in the Schrödinger Maestro suite with the default settings [17]. In the protein optimization initial step in preprocessing was to add hydrogen atoms, take away nonessential hydrogens, and give metals and disulfide bonds zero order bonds. While water molecules that present more than 5.0 Å from any hetero group were eliminated, and missing side chains. Epik was used to assign protonation states at a target pH of 7.0 ± 2.0. All heteroatom groups were left out to keep the protein structure pristine and ready for docking. In final stage refinement, PROPKA was used to optimize hydrogen bond networks and sample water orientations at pH 7.0. Then, the OPLS4 force field was used to minimize the energy of heavy atoms to an RMSD of 0.30 Å. The energy minimized PI3KG structure was then used in molecular docking investigations [18].

After optimizing the proteins to make sure they were stable, a library of natural compounds was prepaired for virtual screening to find possible candidates with good biological activity.

B. Natural Compounds Library

Natural compounds library obtains from the Natural product atlas (https://www.npatlas.org/), npatlas is a curated open-access database of natural substance that have been tested in the lab. The collected compounds were prepared using the LigPrep module of the Schrödinger Suite with default parameter, for the optimization OPLS4 force field were utilized [19]. While module Epik produced possible stereoisomers, ionization states, and tautomeric forms at a physiological pH of 7.0 ± 2.0. To ensure appropriate conformational variation for further molecular docking investigations, up to five low-energy ring conformations were constructed for each molecule [19].

C. Active Site Determination

Structure based drug design mainly focused on accurately finding and describing binding sites on target proteins so that compounds that inhibit biological function can be made in a logical way [20]. This information can be directly exploited for the retrieval and design of new ligands. Structure-based ligand design is an iterative approach. First of all, it requires the crystal structure or a model derived from the crystal structure of a closely related homolog of the target protein, preferentially complexed with a ligand. This complex unravels the binding mode and conformation of a ligand under investigation and indicates the essential aspects determining its binding affinity. It is then used to generate new ideas about ways of improving an existing ligand or of developing new alternative bonding skeletons. Computational methods supplemented by molecular graphics are applied to assist this step of hypothesis generation. The features of the protein binding pocket can be translated into queries used for virtual computer screening of large compound libraries or to design novel ligands de novo. These initial proposals must be confirmed experimentally. Subsequently they are optimized toward higher affinity and better selectivity. The latter aspect is of utmost importance in defining and controlling the pharmacological profile of a ligand. A prerequisite to tailoring selectivity by rational design is a detailed understanding of molecular parameters determining selectivity. Taking examples from current drug development programs (HIV proteinase, t-RNA transglycosylase, thymidylate synthase, thrombin and, related serine proteinases. For PI3KG, we figured out where the active site was by analysis at how the co-crystallized ligand interacted with the amino acid residues around it. PDPsum utilized for the interaction profile analysis, it showed that a few crucial residues help stabilize the ligand by forming various crucial bonds and interactions like hydrogen bonds, hydrophobic interactions etc.

In complex 3-methyl-1-(oxan-4-yl)-8-pyridin-3-yl-imidazo[4,5-c]quinolin-2-one demonstrated stable integration within the PI3KG binding pocket via hydrogen bonding and hydrophobic interactions. A significant hydrogen bond interaction was detected with Trp822 and Asp964, underscoring its essential function in stabilizing the ligand within the active site. The ligand was further stabilized by extensive hydrophobic interactions involving Ile831, Met804, Met953, Ile881, Val882, Ala885, Ile879, Tyr867, and Ile963, which collectively constituted a hydrophobic environment suitable for ligand binding. These interactions play a critical role in keeping the ligand's structure stable and help it bind strongly to the pocket.

Also, the negatively charged residues Glu880 and Asp964 were close to the ligand, which could mean that electrostatic forces could also affect the ligand's orientation and binding stability. The overall interaction pattern indicates that the ligand binds both conserved hydrophobic residues and important polar residues within the PI3KG active site, indicating a well complemented binding strategy (Table I).

TABLE I: PROTEIN-LIGAND INTERACTION ANALYSIS

Hydrogen Bond Interactions				
Ligand	*Protein Residue*	*Chain*	*Interaction Type*	*Distance (Å)*
DD8	Val882 (N)	A	Hydrogen bond	2.89
DD8	Asp964 (N)	A	Hydrogen bond	3.06
Non-Bonded Interaction Summary				
Ligand	*Interacting Residues*	*Nature of Interaction*		
DD8	Met804, Trp812, Ile831, Tyr867, Ile879, Glu880, Val882, Ala885, Met953, Ile963, Asp964	Hydrophobic / van der Waals		
Interaction Summary				
Hydrogen bonds		2		
Non-bonded contacts		49		
Key interacting residues		Val882, Asp964		
Binding pocket nature		Predominantly hydrophobic		

D. Structural Based Virtual Screening

Structure-based virtual screening was performed using the define active site to evaluate the binding affinity of the of natural compounds. In this study, we employed a hierarchical docking system for Structure-based virtual screening, consisting of three stages: High-Throughput Virtual Screening (HTVS), Standard Precision (SP), and Extra Precision (XP). In initial steps at first, HTVS was used to quickly go through the compound library and get rid of compounds with poor affinity. The top 10% of ranking compounds were then moved on to SP and finally XP docking, where the binding evaluation become more and more precise. This progressive screening technique makes predictions more accurate while keeping the process fast. It has been used successfully to target PI3KG [21]. The highest-ranked compounds from the last screening step were tested again to see how well they worked and represent as drugs and to see how well they intact with the human physiology.

E. MM-GBSA Re-Scoring of Glide Docking Results

MM-GBSA were performed utilizing glide module of Schrödinger Suite with default settings and necessary parameters, to glide-generated docked complex for the re-evaluate binding affinity and improve the reliability of the docking results.

F. ADMA Analysis

For the evaluation of pharmacokinetic properties and Drug-likeness of screened compounds we utilized SwissADME web server (http://www.swissadme.ch/). ADME provide information regarding Absorption, Distribution, Metabolism, and Excretion, which is primary properties of drugs. This evaluation offers essential information regarding the appropriateness of compounds for subsequent pharmaceutical development. SwissADME was used to look at important physicochemical and pharmacokinetic factors, such as molecular weight, lipophilicity, water solubility, drug-likeness, and medicinal chemistry features [22]. Additionally, also followed Lipinski's rule of five for the top ranked compounds, in this rule five it was observed that compounds must follow molecular weight (less than 500 Da), logP (less than 5), Fewer than five hydrogen bond donors and fewer than 10 hydrogen bond acceptors. Toxicity prediction was concurrently performed to assess the safety profile of the selected condidate.

G. Toxicity Prediction

ProTox 3.0 web server (https://tox.charite.de/protox3/) evaluate to ident how toxic the lead compounds would be. ProTox 3.0 is a publicly available online platform that integrates molecular similarity assessment with machine learning algorithms to predict various toxicity consequences [23]. In this online web server, we can analyze 61 different endpoints to see how harmful the substance, using this server we can identify acute toxicity (LD_{50}), Mutagenicity, immunotoxicity, cytotoxicity, organ toxicity, and carcinogenicity. This methodology facilitated the prompt identification and elimination of potentially harmful compounds, hence ensuring the selection of candidates with advantageous safety profiles for future examination [23, 24].

III. Results

The primary and principle goal of this study is inhibiting the PI3KG protein function that potentially involved in TNBC progression. Natural compounds were chosen as prospective PI3KG inhibitors due to their structural variety, elevated biocompatibility, and comparatively reduced toxicity relative to synthetic molecules [25]. Natural products have evolved to interact successfully with biological systems, making them particularly valuable scaffolds for drug discovery and development [26, 27]. For the fulfill of this purpose we curated a library of natural compounds from the Natural Products Atlas database and utilized the Glide docking module of the Schrödinger suite to undertake structure based virtual screening against the PI3KG protein, as previously mentioned in the methodology section. For the confirmation the docking approach that were utilized in this study, first a control docking experiment was conducted utilizing the co-crystallized ligand, 3-methyl-1-(oxan-4-yl)-8-pyridin-3-yl-imidazo[4,5-c] quinolin-2-one, associated with PI3KG. Using Glide with the default parameters, the reference ligand was docked in active site of target protein. The docked attitude accurately replicated the essential interactions identified in the crystal structure. Reference compounds bind to the active pocket through certain polar and hydrophobic interactions. Hydrogen bond between the ligand's and residues Trp822 Asp964 is very crucial because it holds the ligand in active site. A polar contact occurs between a heteroaromatic nitrogen of the ligand and Val882. π-type interactions happen between the aromatic ring of the ligand and Tyr867. Ile831, Ile881, Ile879, Ile963, Met804, Met953, Pro810, Trp812, and Phe961 all interaction provide stability in water. Lys833, Lys890, Lys808, Asp950, Asp964, and Glu880 are all charged residues that surround the binding site and help make the electrostatic environment.

The high agreement between the docked pose and the experimentally established binding mode showed that the docking approach was reliable and accurate. Moreover, structural superimposition of the docked and crystallographic

conformations exhibited a significant degree of overlap, further validating the accuracy of the docking process. Additionally, RMSD between the experimental and re-docked ligand conformations was calculated to be less than 2 Å, demonstrating an excellent overlap between the two poses and confirming the high accuracy and reliability of the docking protocol (Fig. 1). This experimental protocol suggest that methodology was subsequently utilized is reliable for the virtual screening of the natural compounds library to find potential PI3KG inhibitors.

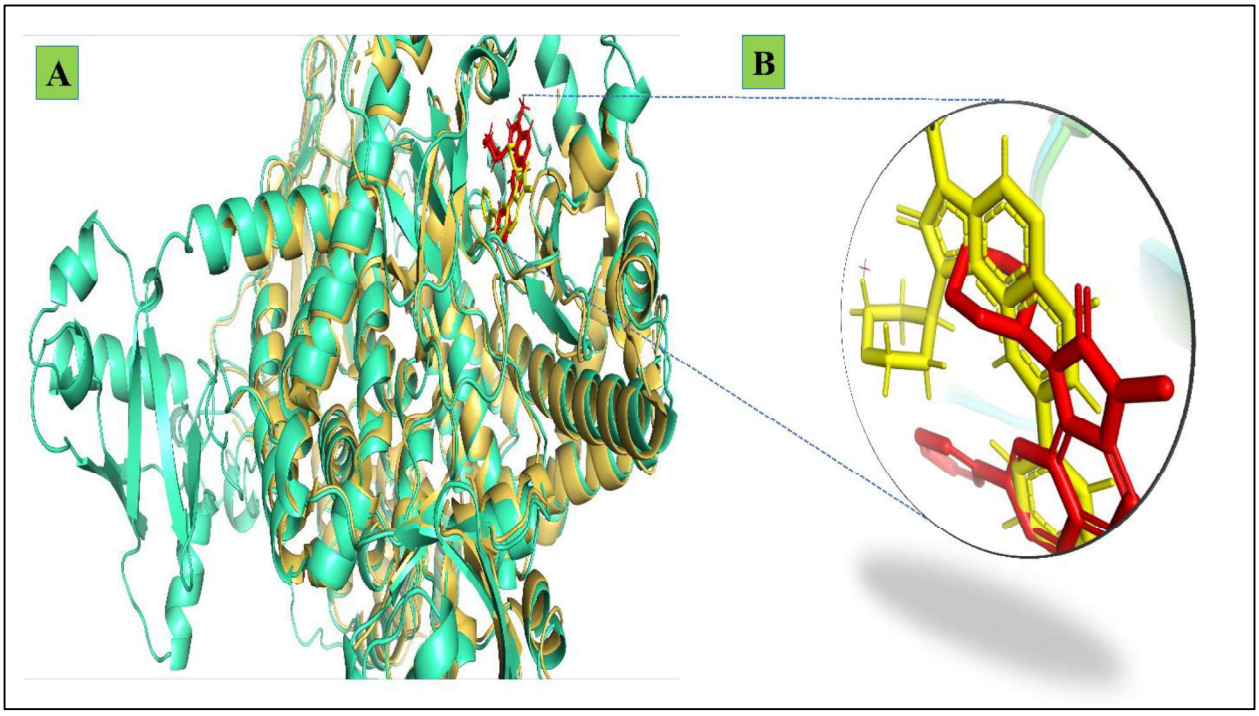

Fig. 1: Validation of the Docking Protocol by Native Ligand Redocking. (A) Superimposed Structure of the Protein Complex Showing the Native Co-Crystal Ligand and the Redocked Ligand within the Same Active Site. (B) Enlarged View of the Active Site Highlighting the Native Co-Crystal Ligand in Yellow Color and the Redocked in Red

In compression of reference compound many natural compounds had a strong binding affinity for the PI3KG protein. The docking scores ranged from -9.016 to -10.01 and the Glide energies ranged from -54.575 to -54.575 kcal/mol, while reference compounds docking score: -5.923 kcal/mol; and Glide energy: -42.091 kcal/mol. Among the top-ranked natural compounds, Phosmidosine B exhibited the strongest binding affinity toward the PI3KG protein, with a docking score of -10.01 and a Glide energy of -60.45 kcal/mol. This was followed by Emodacidamide E, which showed a docking score of -9.69 and a Glide energy of -56.91 kcal/mol, indicating highly favorable binding. Emodacidamide H also demonstrated strong interaction potential, achieving a docking score of -9.62 with a Glide energy of -52.49 kcal/mol. Similarly, Methylinoscavin D displayed a docking score of -9.57 and a Glide energy of -58.71 kcal/mol, suggesting stable binding within the active site. In comparison, 1-hydroxymethyl-8-hydroxy-anthraquinone-3-carboxylic acid showed comparatively moderate binding, with a docking score of -9.54 and a Glide energy of -43.78 kcal/mol (Table II). Overall, these results highlight Phosmidosine B, Emodacidamide E, and Emodacidamide H as the most promising PI3KG inhibitors based on their superior docking performance and favorable energetic profiles. To verify that these top-ranked compounds bind to the same active site as the reference ligand, superimposition analyses were conducted for the five highest scoring complexes. The findings indicated a uniform alignment inside the PI3KG binding pocket and interactions with analogous critical amino acid residues, corroborating a shared binding mechanism (Fig. 2).

Table II: Top Five Compounds and Reference Compounds with Their Docking Score, Glide GScore, Glide Energy and interacting Amino Acids

ID	*Compound_id*	*Compound_name*	*Docking Score*	*Glide Gscore*	*Glide Energy*	*Interacting Amino Acid*
NPA016235	16235	Phosmidosine B	-10.013	-10.013	-60.455	Met804, Ser806, Lys808, Pro810, Trp812, Ile831, Lys833, Tyr867, Ile879, Glu880, Ile881, Val882, Ala885, Thr887, Lys890, Asp950, Asn951, Met953, Phe961, Ile963, Asp964
NPA022342	22342	Emodacidamide E	-9.695	-9.794	-56.918	Ile879, Met953, Thr887, Lys802, Val882, Ile831, Phe961, Met804, Trp812, Asp964, Ile881, Thr886, Ala885, Glu880, Tyr867, Lys890, Ile963.
NPA022345	22345	Emodacidamide H	-9.627	-9.725	-52.498	Met953, Ile831, Lys890, Thr886, Val882, Trp812, Ile963, Ala885, Met804, Asp964, Tyr867, Ile879, Lys802, Phe961, Glu880, Thr887, Ile881.
NPA017182	17182	Methylinoscavin D	-9.576	-9.576	-58.711	Ile879, Tyr867, Phe961, Ile963, Asp964, Met804, Trp812, Glu956, Met953, Ile831, Lys833, Val882, Ile881, Glu880, Lys883, Asp884, Ala885, Thr886
NPA030688	30688	1-hydroxymethyl-8-hydroxy-anthraquinone-3-carboxylic acid	-9.542	-9.543	-43.787	Ile879, Glu880, Ile881, Val882, Ala885, Thr886, Trp812, Met953, Met804, Lys890, Phe961, Ile963, Asp964, Ile831, Tyr867
PubChem CID	134163712	3-methyl-1-(oxan-4-yl)-8-pyridin-3-yl-imidazo[4,5-c]quinolin-2-one.	-5.923	-5.923	-42.091	Ile831, Asp964, Lys808, Tyr867, Val882, Met804, Asp950, Ile963, Trp812, Ser806, Lys833, Glu880, Phe961, Pro810, Thr887, Ala805, Met953, Lys890, Ile879, Ile881.

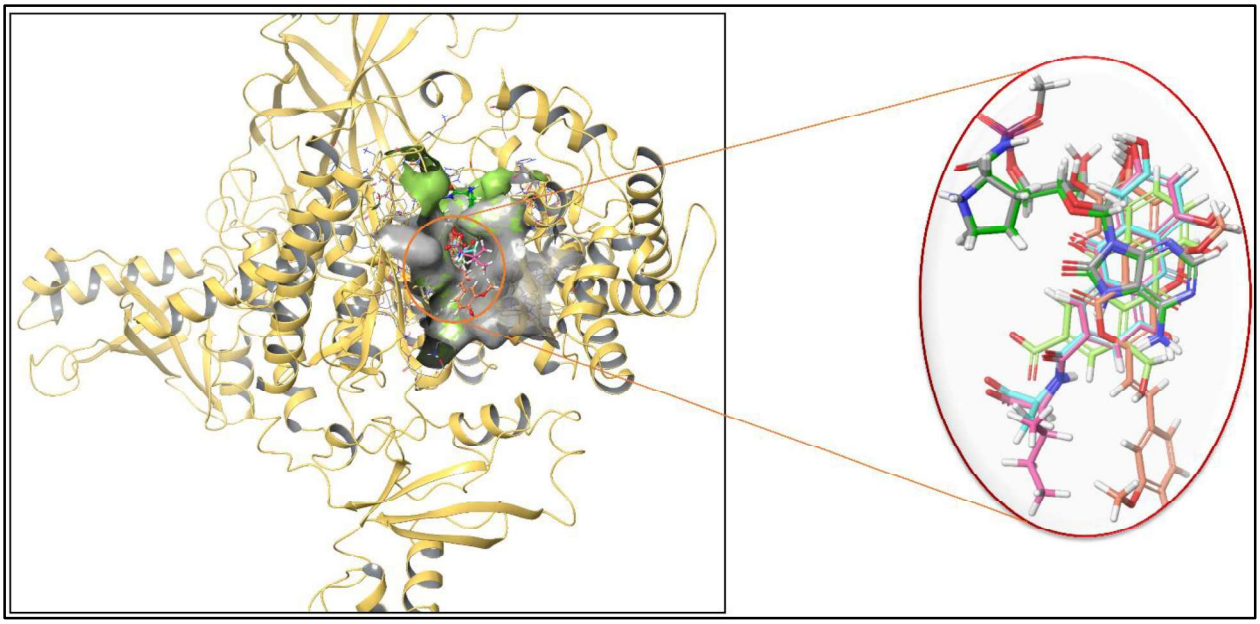

Fig. 2: The Figure Illustrates That Docked Ligands Occupy the Same Active Binding Site of Protein, Indicating a Similar Binding Mode within the Protein

A. Docking Analysis of Phosmidosine B

The 2D interatom diagram of compound Phosmidosine B with target protein 6GQ7 demonstrate that ligands fit well in the active site and is held in place by a strong network of crucial contacts. The ligand makes many strong hydrogen bonds with catalytic and nearby residues, including as Asp950, Asp964, Ser806, Lys808, and Lys833. These interactions are very important for holding the molecule in pocket and keeping its binding specificity. The negatively charged residues Asp950 and Asp964 create stable electrostatic and hydrogen-bond interactions with the polar and positively charged parts of Phosmidosine B. These interactions stabilize the complex strongly.

Also, ionic interactions and salt bridges that involve lysine residues (Lys808, Lys833, and Lys890) make the binding even stronger by stabilizing charged parts of the ligand. The binding pocket is mostly hydrophobic, and residues like Ile831, Ile963, Ile879, Ile881, Val882, Ala885, Met804, Met953, Phe961, Trp812, Tyr867, and Pro810 make a lot of nonpolar interactions that assist hold the ligand in the best shape. These hydrophobic interactions keep the ligand from moving around too much and help it stay in the right place in the pocket.

In addition, the surrounding residues fit the heterocyclic and aromatic parts of Phosmidosine B well, which allows for good π-related interactions and shape complementarity that help keep the ligand in the pocket. The combination of hydrogen bonding, electrostatic interactions, and many hydrophobic contacts makes a binding environment that is very complementary and stable. This shows that Phosmidosine B has a strong affinity for the target protein and shows that it could be a possible inhibitor (Fig. 3-1.a & 1.b).

B. Docking Analysis of Emodacidamide E

The docking interaction results demonstrates that the Emodacidamide E is well accommodated within the binding pocket of target protein by a combination of electrostatic, hydrogen-bonding, aromatic, and hydrophobic interactions. A significant hydrogen bond is detected between the hydroxyl group of the ligand and Asp964, which serves a critical function in anchoring the aromatic core within the active site. Lys890 and Lys802 also form hydrogen bonds with the ligand's amide and carbonyl groups. This helps stabilize the ligand's lower molecular region. Notably, Lys802 also forms a strong ionic connection (salt bridge) with a negatively charged oxygen atom of the ligand, suggesting a large electrostatic anchor that significantly boosts binding affinity. Aromatic scaffold of the ligand participates in advantageous π–π stacking interactions with Tyr867 and Trp812, which assist in maintaining the right orientation of the ligand within the pocket. These interactions are further assisted by a broad hydrophobic environment generated by residues like Ile879, Ile881, Ile963, Ile831, Phe961, Val882, Ala885, Met804, and Met953, which provide van der Waals stability and restrict ligand mobility. Polar residues such as Thr886 and Thr887 are positioned close and likely aid indirectly by preserving a favorable local polarity. This interaction profile supports the substantial binding affinity of the ligand toward the target protein and emphasizes its potential as an effective inhibitor (Fig. 3-2.a & 2.b).

C. Docking Analysis of Emodacidamide H

2D structure analysis revealed that compounds Emodacidamide H binds persistently inside the active site of target protein via a series of essential noncovalent interactions. The ligand's hydroxyl group and Asp964 establish a strong hydrogen bond, which holds the aromatic core in the binding pocket. Numbers of hydrogen bonds like Val882, Ala885, and Lys890 help keep the ligand in pocket. Salt bridge and hydrogen bond with Lys802 that involves the ligand's carboxylate group serves as a large electrostatic anchor and potentially increases binding affinity. Additionally, aromatic scaffold of Emodacidamide H has π–π stacking interactions with Tyr867 and Trp812, which helps it stay in the pocket. These interactions are strengthened by many hydrophobic contacts with nearby residues, such as Ile879, Ile881, Ile963, Ile831, Phe961, Met804, and Met953. These interactions generate a small, stable binding site, which shows that Emodacidamide H has a considerable affinity for PIK3G (Fig. 3-3.a & 3.b).

D. Docking Analysis Methylinoscavin D

Docking analysis indicates that Methylinoscavin D interacts favorably inside the active site of target protein, facilitated by various contact including hydrogen-bond, aromatic, and hydrophobic contacts. Methylinoscavin D hydroxyl groups make important hydrogen bonds with Asp964 and Asp884, which hold the aromatic scaffold in place at the top and bottom of the binding pocket. An extra hydrogen bond with Val882 helps keep the ligand in the right spot along the pocket wall. The aromatic core of Methylinoscavin D interacts with Trp812 in a π–π stacking way, which helps it stay in the right place and stabilize in the binding cavity. The hydrophobic residues that are around the ligand, such as Tyr867, Phe961, Ile879, Ile881, Ile963, Ile831, Met804, and Met953, make many vander Waals interactions that securely hold the ligand in place and limit its movement. Positively charged residues Lys833 and Lys883 are next to each other, which helps with electrostatic complementarity in the pocket. Polar residues like Thr886 help to provide a good local environment.

The strong hydrogen bonds, aromatic stacking, and many hydrophobic interactions all work together to make a stable and complimentary binding environment. This shows that Methylinoscavin D has a considerable binding affinity for the PIK3G active site (Fig. 3-4.a & 4.b).

E. Docking Analysis 1-Hydroxymethyl-8-Hydroxy-Anthraquinone-3-Carboxylic Acid

2D diagram of docked complex shows that, in binding pocket ligand perfectly occupy pocket of target protein, and numbers of hydrogen bonding, electrostatic, and hydrophobic interactions keep it in place. Two hydroxyl groups on the ligand make hydrogen interactions with important residues in the active site. One hydrogen bond is seen with Glu880, and another involves the backbone or side-chain atoms of Ala885 and Val882. This shows that the ligand orientation is strongly stabilized by polar forces. These hydrogen bonds are probably very important for holding the ligand in place in the pocket. Additionally, it was also notice that, strong electrostatic contact between the negatively charged oxygen atom of the ligand's carboxylate group and the positively charged side chain of Lys890. This suggests that a salt bridge has formed, which makes binding stronger. Compounds aromatic rings also take part in π-related interactions with other aromatic residues. Trp812 and Tyr867 make π–π stacking or π–hydrophobic interactions, which are very important for the overall stability of the protein ligands complex. These interactions assist keep the ligand in a perfect shape in the active site of protein. The binding pocket is largely hydrophobic, as shown by the residues around it, which are Ile879, Ile881, Val882, Met804, Met953, Phe961, Ile963, and Ile831. These residues make van der Waals and hydrophobic interactions with the ligand's non-polar parts, making a snug and complimentary space. This interaction profile indicates a robust and selective binding mechanism inside the active site of protein (Fig. 3-5.a & 5.b).

F. Docking Analysis of Reference Compounds

Docking analysis of reference compound and target protein complex show that 3-methyl-1-(oxan-4-yl)-8-pyridin-3-yl-imidazo[4,5-c]quinolin-2-one (reference compound) binds deeply in the active pocket and is held in place by a balanced of various crucial bond and contact like hydrogen bonds and hydrophobic contacts. A significant hydrogen bond is established between the ligand's carbonyl oxygen and Ser806, which probably acts as an anchoring interaction and helps determine the binding orientation. There is also a polar connection between a ring nitrogen atom of the ligand and Val882, which shows that the heteroaromatic moiety is in a good position within the active site of protein. Aromatic interactions also help keep the complex stable. The heteroaromatic ring of the ligand makes π-type connections with Tyr867, which supports strong aromatic stacking or edge-to-face interactions that help keep the ligand in place in the binding pocket.

Moreover, environment around it is mostly hydrophobic, made up of residues like Ile831, Ile881, Ile879, Ile963, Met804, Met953, Pro810, Trp812, and Phe961. These residues make a number of vans der Waals interactions with the reference compounds nonpolar residues, which makes a complementary binding cavity. While charged residues such as Lys833, Lys890, Lys808, Asp950, Asp964, and Glu880 are on the outside of the pocket and not everyone is directly involved in hydrogen bonding, but their closeness significantly suggests that they help shape the electrostatic topography of the active site and indirectly stabilize the compounds (Fig. 3-6.a & 6.b).

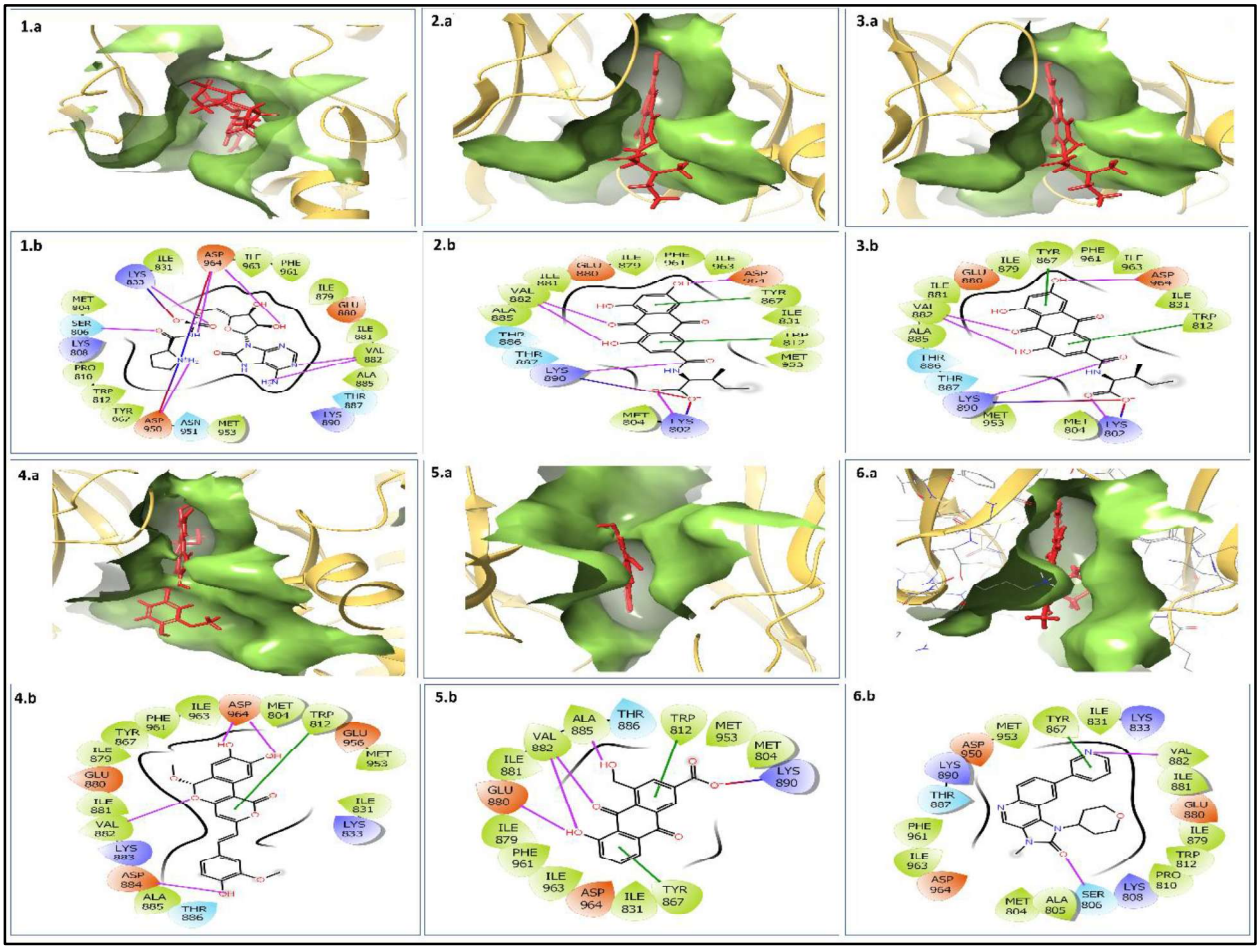

Fig. 3: Three- and Two-Dimensional Docked Complexes of the Natural Compounds, (1.a, 1.b) Phosmidosine B, (2.a, 2.b) Emodacidamide E, (3.a, 3.b) Emodacidamide H, (4.a, 4.b) Methylinoscavin D, (5.a, 5.b) 1-hydroxymethyl-8-hydroxy-anthraquinone-3-carboxylic acid, and (6.a, 6.b) Reference Complex 3-methyl-1-(oxan-4-yl)-8-pyridin-3-yl-imidazo[4,5-c]quinolin-2-one, Exhibit Binding at the Active Site of the PI3KG Protein. 2D Diagram Represent Crucial Interactions, Like Hydrogen Bonds (Pink Arrows), Hydrophobic Interactions (Green), Polar Residues (Blue), Negatively Charged Residues (Red), Glycine (Grey), and Salt Bridges (Red and Blue) for the Docked Complexes of PI3KG with the Selected Natural Compounds

G. MM-GBSA Binding Free Energy Analysis

Docking score results of complexes validate by MM-GBSA binding free energy calculations. Phosmidosine B showed a good binding affinity with a ΔG_bind value of -22.25 kcal/mol. Emodacidamide E and Emodacidamide H, on the other hand, exhibited greater interactions, with corresponding ΔG_bind values of 37.39 and 36.56 kcal/mol. A highly stable and energetically favorable protein-ligand complex was shown by compound 1-hydroxymethyl-8-hydroxy-anthraquinone-3-carboxylic acid most favorable binding free energy (-50.66 kcal/mol) and compound Methylinoscavin D notable increased binding stability (ΔG_bind of 46.41 kcal/mol). The docking results are generally supported by the MM-GBSA analysis, which also identifies all compounds as the most promising binders among the assessed possibilities (Table III).

Table III: MM-GBSA Binding Free Energy of Docked Complexes

Sr. No.	*Compound Compounds*	*(kcal/mol)*
1.	Phosmidosine B	-22.25
2.	Emodacidamide E	-37.39
3.	Emodacidamide H	-36.56
4.	Methylinoscavin D	-46.41
5.	1-hydroxymethyl-8-hydroxy-anthraquinone-3-carboxylic acid	-50.66

H. ADME Profile of Natural Compounds

For the evaluation of ADME and drug-likeness properties of the top five natural compounds utilized SwissADME web server

(Fig. 4). Phosmidosine B has a molecular weight of 459.35 g/mol, it has 31 heavy atoms, 7 rotatable bonds, 11 hydrogen bond acceptors, and 7 hydrogen bond donors. This means that it is very flexible and can form strong hydrogen bonds. But it's very low lipophilicity (cLogP -3.42), high water solubility (ESOL logS 1.53), low gastrointestinal absorption, and two violations of Lipinski's rule of five. These characteristics point to low oral bioavailability and moderate synthetic complexity. However, the molecule comes from naturally, and no major negative effects have been documented, which supports its general safety and biological compatibility. Emodacidamide E molecular weight of 413.38 g/mol and 30 heavy atoms. It also includes 6 rotatable bonds, 8 hydrogen bond acceptors, and 5 donors. It has a high lipophilicity (cLogP 1.73) and a low solubility in water (logS -4.16). It is important to note that it does not violate the RO5 rule, does not pass through the BBB, and has a good synthetic accessibility score of 3.68. This result suggest that it might be used as a drug like molecule. Emodacidamide H has a lower molecular weight of 371.30 g/mol, 27 heavy atoms, and less molecular flexibility, as seen by its 4 rotatable bonds. It has 8 hydrogen bond acceptors and 5 donors, which makes its polarity balanced. It has intermediate lipophilicity (cLogP 0.84) and solubility (logS -3.23), and it follow Lipinski rule, additionally also has a good synthetic accessibility score of 3.19, which means it has drug-like properties.

Methylinoscavin D molecular weight of 410.37 g/mol and 30 heavy atoms. It has 4 rotatable bonds, 8 hydrogen bond acceptors, and 3 donors. It has a higher lipophilicity (cLogP 2.78) and a lower water solubility (logS -4.36), which is what was expected because it is likely to be absorbed well in the stomach. The molecule does not break any RO5 rules and has a synthetic accessibility score of 4.48, which means it is chemically possible and might be used as an oral medication. Lastly, 1-hydroxymethyl-8-hydroxy-anthraquinone-3-carboxylic acid is the smallest molecule in the group. It has a molecular weight of 298.25 g/mol and 22 heavy atoms (compounds structure showed in figure 5). It has only two rotatable bonds, six hydrogen bond acceptors, and three donors, which shows that it is structurally stable and has the best polarity. The chemical has a moderate lipophilicity (cLogP 1.37), a good solubility (logS -3.03), a high gastrointestinal absorption, no RO5 violations, and the best synthetic accessibility score (2.73), which shows that it has a drug-like profile. None of the chemicals were projected to be able to cross the blood-brain barrier, which is a good characteristic because it lowers the chance of side effects in the central nervous system. The ADME analysis shows that the compounds have different molecular sizes, hydrogen-bonding capacities, lipophilicities, solubilities, and pharmacokinetic behaviors. This suggests that they could be good candidates for further development as PIK3G inhibitors (Table IV). All attributes of selected compounds mention in supplementary Table IV.

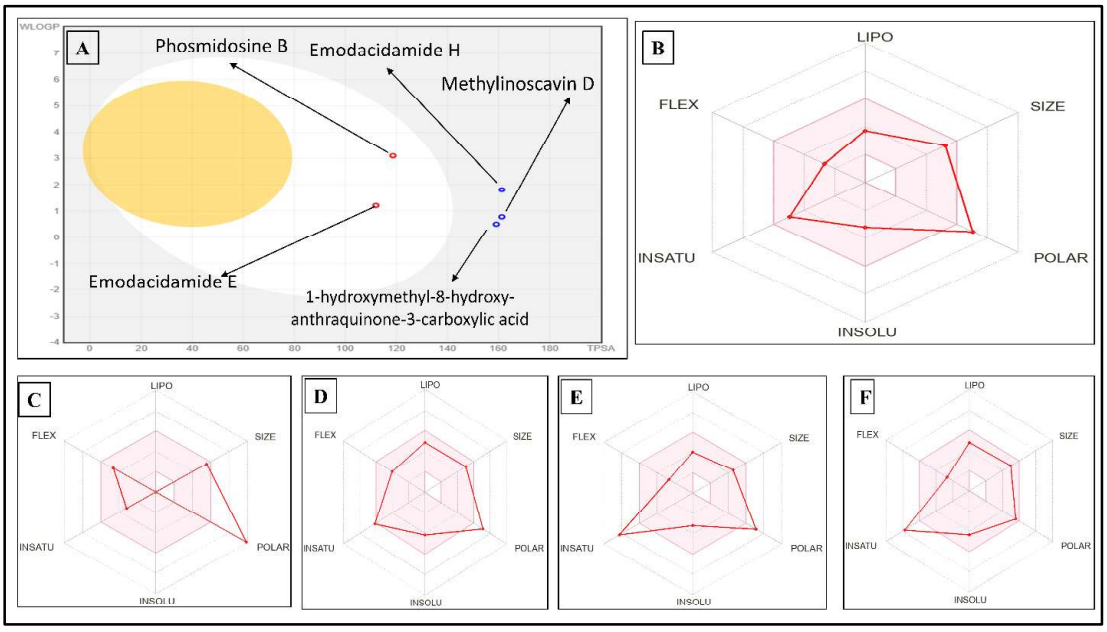

Fig. 4: (A) BOILED-Egg Model Showing the Predicted Pharmacokinetic Properties of the Natural Ligands. The Plot Illustrates the Relationship Between Lipophilicity (WLOGP) and Polarity (TPSA), Where the White Region Represents High Human Intestinal Absorption (HIA) and the Yellow Region Indicates Blood Brain Barrier (BBB) Permeability. Blue Dots Denote P-Glycoprotein Substrates (PGP+), While Red Dots Represent Non-Substrates (PGP−). Most Ligands Fall within the Hia Region with Limited BBB Penetration, Indicating Favorable Oral Bioavailability. Bioavailability Radar Demonstrated Pharmacokinetic Behavior, And Drug-Likeness Properties, (B) Phosmidosine B, (C) Emodacidamide E, (D) Emodacidamide H, (E) Methylinoscavin D, and (F) 1-hydroxymethyl-8-hydroxy-anthraquinone-3-carboxylic acid

Table IV: ADME Attributes of Natural Compounds

Properties		*Phosmidosine B*	*Emodacidamide E*	*Emodacidamide H*	*Methylinoscavin D*	*1-hydroxymethyl-8-hydroxy-anthraquinone-3-carboxylic acid*
Physicochemical properties'	Formula	C15H22N7O8P	C21H19NO8	C18H13NO8	C22H18O8	C16H10O6
	MW (g/mol)	459.35	413.38	371.3	410.37	298.25
	Heavy Atoms	31	30	27	30	22
	Rotatable bonds	7	6	4	4	2
	H-bonds acceptors	11	8	8	8	6
	H-bonds donor	7	5	5	3	3
Lipophilicity	C Log Po/w	-3.42	1.73	0.84	2.78	1.37
Water solubility	ESOL Log S	1.53	-4.16	-3.23	-4.36	-3.03
Pharmacokinetics	GI absorption	Low	Low	Low	High	High
	BBB permeant	No	No	No	No	No
Drug-likeness	RO5 violation	2	0	0	0	0
Medicinal Chemistry	Synthetic accessibility	5.42	3.68	3.19	4.48	2.73

I. Toxicity Profile of Natural Compounds

The toxicity profiles of the top natural compounds were evaluated using predictive toxicity attributes for the figure out how poisonous the chosen compounds were and whether they were safe for further research. Phosmidosine B was expected to be non-toxic for hepatotoxicity, carcinogenicity, immunotoxicity, and cytotoxicity, with mild mutagenicity. It also had a very high LD_{50} value (11,250 mg/kg; toxicity class 6), which means it is very low in acute toxicity. Emodacidamide E and Emodacidamide H exhibited the most advantageous safety profiles, demonstrating inactivity across all toxicity endpoints and being categorized non-toxic (LD_{50} 5,000 mg/kg; class 5). Methylinoscavin D and 1-hydroxymethyl-8-hydroxy-anthraquinone-3-carboxylic acid showed some active immunotoxic or mutagenic predictions, but they did not kill cells. Their LD_{50} values put them in toxicity class 4, which means they are not very toxic. The results show that all of the compounds have acceptable safety profiles and are good candidates for additional pharmacological testing (Table V) All attributes of selected compounds mention in supplementary Table V.

Table V: Toxicity Profiling of Natural Substances

Compound	*Hepatotoxicity*	*Carcinogenicity*	*Immunotoxicity*	*Mutagenicity*	*Cytotoxicity*	*LD_{50} (mg/kg)/ Class*
Phosmidosine B	Inactive (0.61)	Inactive (0.58)	Inactive (0.99)	Active (0.67)	Inactive (0.69)	11250mg/kg (6)
Emodacidamide E	Inactive (0.63)	Inactive (0.56)	Inactive (0.81)	Inactive (0.65)	Inactive (0.62)	5000(5)
Emodacidamide H	Inactive (0.61)	Inactive (0.56)	Inactive (0.91)	Inactive (0.62)	Inactive (0.73)	5000(5)
Methylinoscavin D	Inactive (0.75)	Active (0.51)	Active (0.99)	Active (0.57)	Inactive (0.90)	1500 (4)
1-hydroxymethyl-8-hydroxy-anthraquinone-3-carboxylic acid	Inactive (0.82)	Inactive (0.58)	Active (0.59)	Active (0.72)	Inactive (0.90)	5000(4)

IV. Discussion

To the best of our knowledge, PIK3G has not yet been utilized as a therapeutic target in TNBC using natural compounds, despite the fact that numbers of researches have studies the suppression of well-established breast cancer targets. In this study, we proposed PIK3G as a novel and unexplored target in TNBC by using biocomputational methods to discover and assess natural compounds to inhibit this PIK3G. In this study we utilized Natural Products Atlas library that have thousand compounds, after docking analysis results showed noticeably higher binding affinities for the PI3KG protein than the reference compounds, the screened natural compounds had docking scores between -9.016 and -10.01 kcal/mol and corresponding Glide energies between -54.575 and -60.45 kcal/mol. While reference compounds docking score of -5.923 kcal/mol and a Glide energy of -42.091 kcal/mol, statics showed this is significantly weaker interaction. In top scored compounds we further select five that have highest binding affinity with protein. Among them first compounds Phosmidosine B had the best docking score (-10.01 kcal/mol) and the lowest Glide energy (-60.45 kcal/mol) of all the natural compounds examined, indicating the strongest binding affinity toward PI3KG. These findings show its good inhibitory potential against PI3KG and point to a very persistent and energetically advantageous interaction. Phosmidosine B, that isolated from Streptomyces species, have anticancer and cell growth inhibitory properties. However, Phosmidosine B yet not notice as potential candidate. Phosmidosine B high binding affinity for PI3KG, as shown in this study, is therefore a new in silico result that needs more experimental confirmation [42]. Second molecule Emodacidamide E with a Glide energy of -56.91 kcal/mol and a docking score of -9.69 kcal/mol. Its putative function as an efficient PI3KG inhibitor is supported by the significant negative results, which show strong binding interactions. With a docking score of -9.62 kcal/mol and a glide energy of -52.49 kcal/mol, Emodacidamide H also demonstrated a strong interaction, further validating its advantageous binding within the protein's catalytic region. With a docking score of -9.57 kcal/mol and a glide energy of -58.71 kcal/mol, methylinoscavin D also demonstrated a noteworthy binding affinity, indicating robust accommodation within the PI3KG active site. In contrast, 1-hydroxymethyl-8-hydroxy-anthraquinone-3-carboxylic acid had a greater Glide energy (-43.78 kcal/mol), suggesting substantially lower binding stability, even though it had a respectable docking score (-9.54 kcal/mol). In our best knowledge these compounds yet not utilized as potential inhibitors to breast cancer so they are a novel inhibitor and overall excellent docking scores and advantageous energy profiles, ADME analysis and toxicity prediction of these compounds stood out as the most potential PI3KG inhibitors, Need to more experimental validation and thorough pharmacological research.

V. Conclusion

Breast cancer a heterogenous disease that classified in subtypes among them TNBC one of them, lack of specific receptors makes it untreatable. Several potential targets utilized but yet no any promising target identify. Chemotherapy a satisfactory option but resistance a major challenge, in this study we target a crucial protein PIK3G by natural compounds, PIK3G have role in cancer progression, for the target we utilized a computation-based approach. Results demonstrat that several natural compounds exhibit significantly stronger binding affinity toward the PI3KG protein compared to the reference compound. Among them, Phosmidosine B showed the most favorable docking score and Glide energy, followed by Emodacidamide E, Emodacidamide H, Additionaly Methylinoscavin D and 1-hydroxymethyl-8-hydroxy-anthraquinone-3-carboxylic acid indicating stable and energetically favorable interactions within the PI3KG active site. Additionally, their medicinal properties and toxicity were also investigated. Although Phosmidosine B are known nucleotide antibiotics isolated from Streptomyces species with reported anticancer and cell growth inhibitory activities. Overall, these results suggest that these compounds may serve as promising PI3KG inhibitors, Additional experimental investigations are needed to validate their inhibitory efficacy for their further use.

Declarations

Funding: This research received no external funding.

Authors' Contributions: Conceptualization: PKT& SK; Methodology: PKT& SK; Investigation: PKT& SK; Formal analysis: PKT, SKM & SK; Data curation: PKT& SK; Writing original draft: PKT, SKM & SK; Writing review and editing: PKT, SKM & SK; Supervision and project administration: PKT& SK. All authors approved the final manuscript.

Ethics Statement: All participants provided informed consent prior to participation. Participation was voluntary, and confidentiality of responses was strictly maintained. The study was conducted in accordance with the principles of the Declaration of Helsinki and applicable local regulations.

Conflict of Interest Declaration: The authors declare that they have no affiliations with or involvement in any organization or entity with any financial or non-financial interest in the subject matter or materials discussed in this manuscript.

AI Tool Use Disclosure: AI tools were not used for data generation or analysis. They were used only for language and reference editing. The authors take full responsibility for the final manuscript.

Data Availability: The raw data supporting the conclusions of this article will be made available by the authors, without undue reservation.

Acknowledgments: The authors are highly thankful Sharda University for providing the resources for this work.

References

[1] R. G. do,Nascimento, and K. M. Otoni, "Histological and molecular classification of breast cancer: What do we know?," *Mastology*, vol. 30, pp. 1–8, 2020.

[2] P. Zagami, and L. A. Carey, "Triple negative breast cancer: Pitfalls and progress," *NPJ Breast Cancer*, vol. 8, p. 95, 2022, doi: https://doi.org/10.1038/s41523-022-00468-0.

[3] K. Asleh, N. Riaz, and T. O. Nielsen, "Heterogeneity of triple negative breast cancer: Current advances in subtyping and treatment implications," *J Exp Clin Cancer Res*, vol. 41, p. 265, 2022, doi: https://doi.org/10.1186/s13046-022-02476-1.

[4] Q. Li, Z. Li, T. Luo, and H. Shi, "Targeting the PI3K/AKT/mTOR and RAF/MEK/ERK pathways for cancer therapy," *Mol Biomed*, vol. 3, p. 47, 2022, doi: https://doi.org/10.1186/s43556-022-00110-2.

[5] M. K. Elbashir, M. Mohammed, H. Mwambi, B. Omolo, M. K. Elbashir, M. Mohammed *et al.*, "Identification of hub genes associated with breast cancer using integrated gene expression data with protein-protein interaction network," *Appl Sci*, vol. 13, 2023, doi: https://doi.org/10.3390/app13042403.

[6] E. Hirsch, V. L. Katanaev, C. Garlanda, O. Azzolino, L. Pirola, L. Silengo *et al.,* "Central role for G protein-coupled phosphoinositide 3-kinase γ in inflammation," *Science*, vol. 287, pp. 1049–1053, 2000, doi: https://doi.org/10.1126/science.287.5455.1049.

[7] G. P. Mognol, A. Ghebremedhin, and J. A.Varner, "Targeting PI3Kγ in cancer," *Trends Cancer*, vol. 11, pp. 462–474, 2025, doi: https://doi.org/10.1016/j.trecan.2025.01.008.

[8] A. Ghebremedhin, and J. A. Varner, "PI3Kγ in tumour inflammation: Bridging immune response and cancer progression - A mini-review," *Immunology*, vol. 176, pp. 215–223, 2025, doi: https://doi.org/10.1111/imm.13959.

[9] D. A. Fruman, R. E. Meyers, and L. C. Cantley, "PHOSPHOINOSITIDE KINASES," *Annu Rev Biochem*, vol. 67, pp. 481–507, 1998, doi: https://doi.org/10.1146/annurev.biochem.67.1.481.

[10] I. Vivanco, and C. L. Sawyers, "The phosphatidylinositol 3-Kinase–AKT pathway in human cancer," *Nat Rev Cancer*, vol. 2, pp. 489–501, 2002, doi: https://doi.org/10.1038/nrc839.

[11] D. Huang, J. Yang, Q. Zhang, X. Zhou, Y. Wang, Z. Shang *et al.*, "Design, synthesis, and biological evaluation of 2,4-dimorpholinopyrimidine-5-carbonitrile derivatives as orally bioavailable PI3K inhibitors," *Front Pharmacol*, vol. 15, 2024, doi: https://doi.org/10.3389/fphar.2024.1467028.

[12] L. S. Carnevalli, M. A. Taylor, M. King, A. M. L. Coenen-Stass, A. M. Hughes, S. Bell *et al.,* "Macrophage activation status rather than repolarization is associated with enhanced checkpoint activity in combination with PI3Kγ inhibition," *Mol Cancer Ther*, vol. 20, pp. 1080–1091, 2021, doi: https://doi.org/10.1158/1535-7163.MCT-20-0961.

[13] B. Chopra, and A. K. Dhingra, "Natural products: A lead for drug discovery and development," *Phytother Res*, vol. 35, pp. 4660–4702, 2021, doi: https://doi.org/10.1002/ptr.7099.

[14] S. Mitra, and R. Dash, "Natural products for the management and prevention of breast cancer," *Evid Based Complement Alternat Med*, p. 8324696, 2018, doi: https://doi.org/10.1155/2018/8324696.

[15] C. Yang, A. Alam, F. A. Alhumaydhi, M. S. Khan, S. A. Alsagaby, W. A. Abdulmonem *et al.,* "Bioactive phytoconstituents as potent inhibitors of Tyrosine-Protein Kinase Yes (YES1): Implications in anticancer therapeutics," *Molecules*, vol. 27, 2022, doi: https://doi.org/10.3390/molecules27103060.

[16] B. Noel, S. K. Singh, J. W. Lillard, and R. Singh, "Role of natural compounds in preventing and treating breast cancer," *Front Biosci Sch Ed*, vol. 12, pp. 137–160, 2020, doi: https://doi.org/10.2741/s544.

[17] A. Q. Khalid, S. Bhuvanendran, K. B. Magalingam, P. Ramdas, Y. K. Liew, and A. K. Radhakrishnan, "Protocol for predicting γ-tocotrienol and δ-tocotrienol binding to colorectal cancer-related proteins using Schrödinger's maestro and glide," *STAR Protoc,* vol. 6, p. 104144, 2025, doi: https://doi.org/10.1016/j.xpro.2025.104144.

[18] J. J. Sahayarayan, K. S. Rajan, R. Vidhyavathi, M. Nachiappan, D. Prabhu, S. Alfarraj *et al.*, "*In-silico* protein-ligand docking studies against the estrogen protein of breast cancer using pharmacophore based virtual screening approaches," *Saudi J Biol Sci*, vol. 28, pp. 400–407, 2021, doi: https://doi.org/10.1016/j.sjbs.2020.10.023.

[19] A. J. Yusuf, M. I. Abdullahi, I. Nasir, A. Yunusa, A. M. Musa, A. A. Muhammad *et al.,* "Identification of possible antimalarial constituent(s) from the leaves of *Ochna kibbiensis*: A phytochemical, *in vivo* and

in silico approaches," *Phytomedicine Plus*, vol. 5, p. 100764, 2025, doi: https://doi.org/10.1016/j.phyplu.2025.100764.

[20] G. Klebe, "Recent developments in structure-based drug design," *J Mol Med*, vol. 78, pp. 269–281, 2000, doi: https://doi.org/10.1007/s001090000084.

[21] P. Kumar Tiwari, M. Chouhan, R. Mishra, S. Gupta, A. A. Chaudhary, M. Al-Zharani *et al.,* "Structure-based virtual screening methods for the identification of novel phytochemical inhibitors targeting furin protease for the management of COVID-19," *Front Cell Infect Microbiol*, vol. 14, 2024, doi: https://doi.org/10.3389/fcimb.2024.1391288.

[22] A. Daina, O. Michielin, and V. Zoete, "SwissADME: A free web tool to evaluate pharmacokinetics, drug-likeness and medicinal chemistry friendliness of small molecules," *Sci Rep*, vol. 7, p. 42717, 2017, doi: https://doi.org/10.1038/srep42717.

[23] P. Banerjee, E. Kemmler, M. Dunkel, and R. Preissner, "ProTox 3.0: A webserver for the prediction of toxicity of chemicals," *Nucleic Acids Res*, vol. 52, pp. W513–W520, 2024, doi: https://doi.org/10.1093/nar/gkae303.

[24] M. Kumar, R. Dubey, P. Kumar Shukla, D. Dayal, Kumar K. Chaubey, L.-W. Tsai *et al.,* "Identification of small molecule inhibitors of RAD52 for breast cancer therapy: In silico approach," *J Biomol Struct Dyn*, vol. 42, pp. 4605–4618, 2024, doi: https://doi.org/10.1080/07391102.2023.2220822.

[25] E. C. Barnes, R. Kumar, and R. A. Davis, "The use of isolated natural products as scaffolds for the generation of chemically diverse screening libraries for drug discovery," *Nat Prod Rep*, vol. 33, pp. 372–381, 2016, doi: https://doi.org/10.1039/C5NP00121H.

[26] C. Barba-Ostria, S. E. Carrera-Pacheco, R. Gonzalez-Pastor, J. Heredia-Moya, A. Mayorga-Ramos, C. Rodríguez-Pólit *et al.,* "Evaluation of biological activity of natural compounds: Current trends and methods," *Molecules*, vol. 27, 2022, doi: https://doi.org/10.3390/molecules27144490.

[27] Y. Ding, X. Xue, Y. Ding, and X. Xue, "Medicinal chemistry strategies for the modification of bioactive natural products," *Molecules*, vol. 29, 2024, doi: https://doi.org/10.3390/molecules29030689.

[28] A. Szymiczek, A. Lone, and M. R. Akbari, "Molecular intrinsic versus clinical subtyping in breast cancer: A comprehensive review," *Clin Genet*, vol. 99, pp. 613–637, 2021, doi: https://doi.org/10.1111/cge.13900.

[29] A. Mackay, B. Weigelt, A. Grigoriadis, B. Kreike, R. Natrajan, R. A'Hern *et al.,* "Microarray-based class discovery for molecular classification of breast cancer: Analysis of interobserver agreement," *JNCI J Natl Cancer Inst*, vol. 103, pp. 662–673, 2011, doi: https://doi.org/10.1093/jnci/djr071.

[30] P. Gazinska, A. Grigoriadis, J. P. Brown, R. R. Millis, A. Mera, C. E. Gillett *et al.,* "Comparison of basal-like triple-negative breast cancer defined by morphology, immunohistochemistry and transcriptional profiles," *Mod Pathol*, vol. 26, pp. 955–966, 2013, doi: https://doi.org/10.1038/modpathol.2012.244.

[31] R. Yang, Y. Li, H. Wang, T. Qin, X. Yin, and X. Ma, "Therapeutic progress and challenges for triple negative breast cancer: Targeted therapy and immunotherapy," *Mol Biomed*, vol. 3, p. 8, 2022, doi: https://doi.org/10.1186/s43556-022-00071-6.

[32] L. Wein, and S. Loi, "Mechanisms of resistance of chemotherapy in early-stage Triple Negative Breast Cancer (TNBC)," *The Breast,* vol. 34, pp. S27–S30, 2017, doi: https://doi.org/10.1016/j.breast.2017.06.023.

[33] Y. Li, Z. Zhan, X. Yin, S. Fu, and X. Deng, "Targeted therapeutic strategies for triple-negative breast cancer," *Front Oncol*, vol. 11, 2021, doi: https://doi.org/10.3389/fonc.2021.731535.

[34] G. Barchiesi, M. Roberto, M. Verrico, P. Vici, S. Tomao, and F. Tomao, "Emerging role of PARP inhibitors in metastatic triple negative breast cancer: Current scenario and future perspectives," *Front Oncol,* vol. 11, 2021, doi: https://doi.org/10.3389/fonc.2021.769280.

[35] X. Chen, L. Feng, Y. Huang, Y. Wu, N. Xie, X. Chen *et al.,* "Mechanisms and strategies to overcome PD-1/PD-L1 blockade resistance in triple-negative breast cancer," *Cancers*, vol. 15, 2022, doi: https://doi.org/10.3390/cancers15010104.

[36] A. Gucalp, and T. A. Traina, "Targeting the androgen receptor in triple-negative breast cancer," *Curr Probl Cancer*, vol. 40, pp. 141–150, 2016, doi: https://doi.org/10.1016/j.currproblcancer.2016.09.004.

[37] D Massihnia, A Galvano, D Fanale, A Perez, M Castiglia, L Incorvaia *et al.,* "Triple negative breast cancer: shedding light onto the role of pi3k/akt/mtor pathway," *Oncotarget*, vol. 7, pp. 60712–60722, 2016, doi: https://doi.org/10.18632/oncotarget.10858.

[38] H. Tang, K. Ren, G. Wang, R. Zhang, and L. Zhang, "Computational design of phosphoinositide 3-kinase gamma (PI3Kg) inhibitors as a newer therapy for rheumatoid arthritis," *Trop J Pharm Res,* vol. 20, pp. 775–781, 2021, doi: https://doi.org/10.4314/tjpr.v20i4.17.

[39] J. D. Venable, M. K. Ameriks, J. M. Blevitt, R. L. Thurmond, and W.-P. Fung-Leung, "Phosphoinositide 3-kinase gamma (PI3Kγ) inhibitors for the treatment

of inflammation and autoimmune disease," *Recent Pat Inflamm Allergy Drug Discov,* vol. 4, pp. 1–15, 2010, doi: https://doi.org/10.2174/187221310789895603.

[40] H. Ellis, and C. X. Ma, "PI3K inhibitors in breast cancer therapy," *Curr Oncol Rep*, vol. 21, p. 110, 2019, doi: https://doi.org/10.1007/s11912-019-0846-7.

[41] J. Chang, L. Hong, Y. Liu, Y. Pan, H. Yang, W. Ye *et al.*, "Targeting PIK3CG in combination with paclitaxel as a potential therapeutic regimen in claudin-low breast cancer," *Cancer Manag Res,* vol. 12, pp. 2641–2651, 2020, doi: https://doi.org/10.2147/CMAR.S250171.

[42] T. Moriguchi, N. Asai, K. Okada, K. Seio, T. Sasaki, and M. Sekine, "First synthesis and anticancer activity of phosmidosine and its related compounds," *J Org Chem,* vol. 67, pp. 3290–3300, 2002, doi: https://doi.org/10.1021/jo016176g.